19. To be published.
20. The oxidation rate is given by:
Rate $= k[XNAH\text{-}Cu^{2+}]$
$= kK(1-f_{XNAH})(1-f_{XNAH}[XNAH]_t/[Cu^{2+}]_t) \times [XNAH]_t [Cu^{2+}]_t$
$= k_{Cu}[XNAH]_t [Cu^{2+}]_t$
Thus the apparent second order oxidation rate constant $k_{Cu}$ decreases as the complexed fraction of XNAH, $f_{XNAH}$ increases for a given complex formation constant K. The k is the intrinsic electron transfer rate constant of the complex and $k_{Cu}$ becomes kK as $f_{XNAH} \rightarrow 0$.
21. At condition of $[Cu^{2+}] \gg [XNAH]$, the concentration of XNAH-$Cu^{2+}$ complex is proportional to total concentration of XNAH by $[XNAH\text{-}Cu^{2+}] = K[Cu^{2+}][XNAH]_t/(1 + K[Cu^{2+}])$. Thus the first order kinetics in XNAH expressed in eq. 1 is still valid.

# Four Crystal Structures of Dehydrated $Ag^+$ and $Tl^+$ Exchanged Zeolite A, $Ag_{12-x}Tl_x$-A, x = 2,3,4, and 5

**Duk Soo Kim, Seong Hwan Song*, and Yang Kim***

*Department of Chemistry, Cheju National University, Cheju 690-756*
**Department of Chemistry, Pusan National University, Pusan 609-745.* *Received April 15, 1988*

Four crystal structures of dehydrated Ag(I) and Tl(I) exchanged zeolite A, $Ag_{12-x}Tl_xA$, x = 2,3,4, and 5, have been determined by single-crystal x-ray diffraction techniques. Their structures were solved and refined in the cubic space group *Pm3m* at 21(1) °C. All crystals were ion exchanged in flowing streams of mixed $AgNO_3$ and $TlNO_3$ aqueous solution, followed by dehydration at 350 °C and $2 \times 10^{-6}$ Torr for 2 days. In all of these structures, one-sixth of the sodalite units contain octahedral hexasilver clusters at their centers and eight $Ag^+$ ions are found on threefold axes, each nearly at the center of a 6-oxygen ring. The hexasilver cluster is stabilized by coordination to eight $Ag^+$ ions. The Ag-Ag distance in the cluster, ca. 2.92Å, is near the 2.89 Å bond length in silver metal. The remaining five-sixths of the sodalite units are empty of silver species. The first three $Tl^+$ ions per unit cell preferentially associate with 8-oxygen rings, and additional $Tl^+$ ions, if present, are found on threefold axes in the large cavity.

## Introduction

The properties of zeolites are sensitive to their cationic contents. A knowledge of the siting of these cations within a zeolite framework can provide a structural basis for understanding these properties. Thus far, the structures of $Ag^+$ [1,2], $K^+$ [3,4], $Rb^+$ [5], $Cs^+$ [6], $Tl^+$ [7], Mn(II) [8,9], Co(II) [9-12], Ni(II) [9], Zn (II) [9,13], $Ca^{2+}$ [14], and Eu(II) [15] exchanged zeolite A[16] have been determined crystallographically.

Recently several crystal structures of fully $Ag^+$-exchanged zeolite A were determined.[17] Fully dehydrated $Ag_{12}$-A contains silver atoms, probably as hexasilver molecules centered within some of its sodalite cavities. Hexasilver is stabilized by coordination to eight $Ag^+$ ions very near the centers of the 6-oxygen rings on threefold axes.[2,17] Hermerschmidt and Haul identified $Ag_6^{n+}$ (n<6) clusters in the sodalite cavity of dehydrated $Ag^+$-exchanged zeolite A using epr spectroscopy.[18] Their results were verified by Grobet and Schoonheydt[19] and reverified by the careful work of Morton and Preston who did epr measurements on isotropically pure samples of $Ag_{12}$-A[20].

The present study has been initiated to investigate the cation positions in the crystal structures of variously $Ag^+$ and $Tl^+$ exchanged zeolite A. It would be interesting to learn how different numbers of exchanged $Tl^+$ ions arrange themselves in the zeolite framework. Furthermore, because of the high scattering powers of $Tl^+$ and $Ag^+$, precise and reliable crystallographic determinations should be easy to achieve. The present work is preliminary to later studies of the crystal structure of $Ag_{12-x}Tl_x$-A treated with $H_2$ or other guest molecules.

**Table 1. A Summary of Experimental Results**

| Crystal | Zeolite Cation Composition | Ion Exchange Mole ratio ($AgNO_3$:$TlNO_3$) | Ion Exchange Period | Dehydration Temp. (°C) | Dehydration Period (days) | Dehydration Pressure (Torr.) | Unit Cell Constant(Å) | Number of[a] Observed Reflections | $R_1$ | $R_2$ |
|---|---|---|---|---|---|---|---|---|---|---|
| 1 | $Ag_{10}Tl_2$-A | 5:1 | 2 days | 350 | 2 | $2 \times 10^{-6}$ | 12.300(2)[b] | 302 | 0.054 | 0.057 |
| 2 | $Ag_9Tl_3$-A | 1.9:1 | 2 days | 350 | 2 | $2 \times 10^{-6}$ | 12.243(2) | 256 | 0.070 | 0.070 |
| 3 | $Ag_8Tl_4$-A | 1:1 | 2 days | 350 | 2 | $2 \times 10^{-6}$ | 12.281(1) | 377 | 0.067 | 0.067 |
| 4 | $Ag_7Tl_5$-A | 1:5 | 2 days | 350 | 2 | $2 \times 10^{-6}$ | 12.263(1) | 323 | 0.055 | 0.063 |

[a]Only those reflections for which $I > 3\sigma(I)$ were considered observed. [b]The number in parentheses is the esd in the units of the least significant digit given.

**Table 2. [a]Positional, Thermal, and Occupancy Parameters**

Crystal 1, $Ag_{10}Tl_2$-A

| Atom | Wyc. Posi. | x | y | z | $\beta_{11}$[b] | $\beta_{22}$ | $\beta_{33}$ | $\beta_{12}$ | $\beta_{13}$ | $\beta_{23}$ | occupancy[c] varied | fixed |
|---|---|---|---|---|---|---|---|---|---|---|---|---|
| (Si,Al) | 24(k) | 0 | 1834(3) | 3699(2) | 18(2) | 15(2) | 10(1) | 0 | 0 | 2(4) | | 24.0 |
| O(1) | 12(h) | 0 | 2170(10) | 5000 | 70(10) | 40(10) | 15(7) | 0 | 0 | 0 | | 12.0 |
| O(2) | 12(i) | 0 | 2968(7) | 2968(7) | 28(7) | 23(4) | 23(4) | 0 | 0 | 20(10) | | 12.0 |
| O(3) | 24(m) | 1120(5) | 1120(5) | 3381(7) | 32(3) | 32(3) | 39(6) | 40(10) | 22(8) | 22(8) | | 24.0 |
| Ag(1) | 8(g) | 1916(2) | 1916(2) | 1916(2) | 75(6) | 75(6) | 75(6) | 100(2) | 100(2) | 100(2) | 7.9(2) | 8.0 |
| Ag(4) | 24(m) | 730(70) | 4180(40) | 4180(40) | 240(80) | 280(50) | 280(50) | -190(70) | -190(70) | -200(100) | 1.1(1) | 1.0 |
| Tl(2) | 12(i) | 0 | 4421(7) | 4721(7) | 132(8) | 70(6) | 190(20) | 0 | 0 | -120(1) | 1.9(2) | 2.0 |
| Ag(3) | 6(e) | 0 | 0 | 1690(20) | 71(8) | 71(8) | 70(10) | 0 | 0 | 0 | 0.7(1) | 1.0 |

Crystal 2, $Ag_9Tl_3$-A

| Atom | Wyc. Posi. | x | y | z | $\beta_{11}$[b] | $\beta_{22}$ | $\beta_{33}$ | $\beta_{12}$ | $\beta_{13}$ | $\beta_{23}$ | occupancy[c] varied | fixed |
|---|---|---|---|---|---|---|---|---|---|---|---|---|
| (Si,Al) | 24(k) | 0 | 1837(4) | 3698(3) | 29(2) | 30(2) | 13(2) | 0 | 0 | 4(5) | | 24.0 |
| O(1) | 12(h) | 0 | 2130(20) | 5000 | 50(10) | 60(20) | 40(10) | 0 | 0 | 0 | | 12.0 |
| O(2) | 12(i) | 0 | 2970(10) | 2970(10) | 50(10) | 33(7) | 33(7) | 0 | 0 | 30(20) | | 12.0 |
| O(3) | 24(m) | 1122(7) | 1122(7) | 3350(10) | 41(5) | 41(5) | 6(10) | 30(10) | 20(10) | 20(10) | | 24.0 |
| Ag(1) | 8(g) | 1894(3) | 1894(3) | 1894(3) | 96(1) | 96(1) | 96(1) | 135(3) | 135(3) | 135(3) | 6.4(2) | 6.5 |
| Ag(2) | 8(g) | 1320(8) | 1320(8) | 1320(8) | 49(4) | 49(4) | 49(4) | 50(10) | 50(10) | 50(10) | 1.4(2) | 1.5 |
| Tl(2) | 12(i) | 0 | 4556(4) | 4556(4) | 178(9) | 136(5) | 136(5) | 0 | 0 | -163(9) | 3.0(1) | 3.0 |
| Ag(3) | 6(e) | 0 | 0 | 1730(20) | 60(9) | 60(9) | 120(2) | 0 | 0 | 0 | 0.8(1) | 1.0 |

Crystal 3, $Ag_8Tl_4$-A

| Atom | Wyc. Posi. | x | y | z | $\beta_{11}$[b] | $\beta_{22}$ | $\beta_{33}$ | $\beta_{12}$ | $\beta_{13}$ | $\beta_{23}$ | occupancy[c] varied | fixed |
|---|---|---|---|---|---|---|---|---|---|---|---|---|
| (Si,Al) | 24(k) | 0 | 1840(3) | 3698(2) | 22(2) | 23(2) | 12(1) | 0 | 0 | 3(3) | | 24.0 |
| O(1) | 12(h) | 0 | 2160(10) | 5000 | 48(9) | 70(10) | 20(7) | 0 | 0 | 0 | | 12.0 |
| O(2) | 12(i) | 0 | 2957(7) | 2957(7) | 28(7) | 29(4) | 29(4) | 0 | 0 | 20(10) | | 12.0 |
| O(3) | 24(m) | 1137(5) | 1137(5) | 3381(7) | 32(3) | 32(3) | 47(6) | 15(9) | 14(7) | 14(7) | | 24.0 |
| Ag(1) | 8(g) | 1901(2) | 1901(2) | 1901(2) | 46(1) | 46(1) | 46(1) | 60(2) | 60(2) | 60(2) | 4.7(1) | 5.0 |
| Ag(2) | 8(g) | 1580(10) | 1580(10) | 1580(10) | 192(4) | 192(4) | 192(4) | 301(9) | 301(9) | 301(9) | 2.1(3) | 2.0 |
| Tl(1) | 8(g) | 2490(10) | 2490(10) | 2490(10) | 211(6) | 211(6) | 211(6) | 280(10) | 280(10) | 280(10) | 1.2(2) | 1.0 |
| Tl(2) | 12(i) | 0 | 4550(3) | 4550(3) | 151(6) | 125(3) | 125(3) | 0 | 0 | -170(6) | 3.2(3) | 3.0 |
| Ag(3) | 6(e) | 0 | 0 | 1670(10) | 62(7) | 62(7) | 40(10) | 0 | 0 | 0 | 0.6(2) | 1.0 |

Crystal 4, $Ag_7Tl_5$-A

| Atom | Wyc. Posi. | x | y | z | $\beta_{11}$[b] | $\beta_{22}$ | $\beta_{33}$ | $\beta_{12}$ | $\beta_{13}$ | $\beta_{23}$ | occupancy[c] varied | fixed |
|---|---|---|---|---|---|---|---|---|---|---|---|---|
| (Si,Al) | 24(k) | 0 | 1836(3) | 3693(2) | 19(2) | 20(2) | 15(2) | 0 | 0 | 4(3) | | 24.0 |
| O(1) | 12(h) | 0 | 2170(10) | 5000 | 60(10) | 50(10) | 17(7) | 0 | 0 | 0 | | 12.0 |
| O(2) | 12(i) | 0 | 2979(7) | 2979(7) | 37(8) | 22(4) | 22(4) | 0 | 0 | 30(10) | | 12.0 |
| O(3) | 24(m) | 1123(5) | 1123(5) | 3334(7) | 38(4) | 38(4) | 40(6) | 30(10) | 6(8) | 6(8) | | 24.0 |
| Ag(1) | 8(g) | 1892(2) | 1892(2) | 1892(2) | 71(1) | 71(1) | 71(1) | 107(2) | 107(2) | 107(2) | 5.1(2) | 5.0 |
| Ag(2) | 8(g) | 1170(10) | 1170(10) | 1170(10) | 96(6) | 96(6) | 96(6) | 120(20) | 120(20) | 120(20) | 0.9(2) | 1.0 |
| Tl(1) | 8(g) | 2592(2) | 2592(2) | 2592(2) | 35(1) | 35(1) | 35(1) | -3(2) | -3(2) | -3(2) | 2.2(1) | 2.0 |
| Tl(2) | 24(k) | 0 | 4388(4) | 4725(4) | 172(6) | 34(3) | 73(7) | 0 | 0 | -27(6) | 2.9(2) | 3.0 |
| Ag(3) | 6(e) | 0 | 0 | 1650(20) | 110(20) | 110(20) | 80(20) | 0 | 0 | 0 | 0.7(2) | 1.0 |

[a]Positional and isotropic thermal parameters are given $\times 10^4$. Numbers in parentheses are the esd's in units of the least significant digit given for the corresponding parameter. [b]The anisotropic temperature factor = $\exp[-(\beta_{11}h^2 + \beta_{22}k^2 + \beta_{33}l^2 + \beta_{12}hk + \beta_{13}hl + \beta_{23}kl)]$. [c]Occupancy factors given as the number of atoms or ions per unit cell. Occupancy for (Si) = 12; occupancy for (Al) = 12.

## Experimental

Crystals of zeolte 4A were prepared by Charnell's method.[21] A single crystal about 0.08 mm on an edge was lodged in a fine glass capillary. To prepare $Ag^+$ and $Tl^+$ ion exchanged zeolite A crystals, variously mixed exchange solutions of $AgNO_3$ and $TlNO_3$ with a total concentration of 0.05M were used (see Table 1). The exchange was then performed by flow methods; the solution was allowed to flow past the crystal at a velocity of approximately 1.0 cm/sec for 2 days at 24(1) °C. Each crystal was evacuated at 350 °C and $2 \times 10^{-6}$ Torr for 48 hours. After cooling to room temperature, each crystal, still under vacuum, was sealed in its capillary by torch. Subsequent diffraction experiments were performed at 21(1) °C. The cubic space group *Pm3m* (no systematic absences) was used for reasons discussed previously.[22-24] Preliminary crystallographic experiments and subsequent data collection were performed with an automated, four circle Enraf-Nonius CAD-4 diffractometer, equipped with a graphite monochromator. Mo $K_\alpha$ radiation was used for all experiments ($K_{\alpha1}$, $\lambda = 0.70930$Å; $K_{\alpha2}$, $\lambda = 0.71359$Å). The cubic unit cell constants, as determined by a least-squares refinement of 25 intense reflections for which $18° < 2\theta < 24°$, are shown in Table 1.

Reflections from two intensity-equivalent regions of reciprocal space (*hkl*, $h<k<l$ and *lhk*, $l<h<k$) were examined using the $\omega$-$2\theta$ scan technique. The data were collected using variable scan speeds. The intensities of three reflections in diverse regions of reciprocal space were recorded after every three hours to monitor crystal and x-ray source stability. Only small, random fluctuations of these check reflections were noted during the course of data collection.

The raw data for each region were corrected for Lorentz and polarization effects, including that due to incident beam monochromatization; the reduced intensities were merged by the computer program, PAINT.[25] An absorption correction was judged to be unimportant[26], and was not applied. Only the observed reflections, those whose net counts exceeded three times their corresponding esd's,were used in structure solution and refinement.The number of reflections used in structural analysis for each crystal is given in Table 1.

## Structure Determination

All structure calculations were done using the Structure Determination Package(SDP)[25] programs supplied by Enraf-Nonius.

Crystal 1. Full matrix least-squares refinement was initiated using the atomic parameters of the framework atoms [(Si,Al), O(1), O(2), and O(3)] and of the $Ag^+$ ions in $Ag_{12}$-A.[2,27] Anisotropic refinement of the framework atoms and Ag(1) (see Table 2) converged to an $R_1$ index, $(\Sigma||F_o|-|F_c||/\Sigma F_o)$, of 0.180 and a weighted $R_2$ index, $(\Sigma w(F_o-|F_c|)^2/\Sigma wF_o^2)^{1/2}$, of 0.239. A difference Fourier synthesis revealed large and distinct peaks at (0.0,0.0,0.166) with a height of 7.0(4)eÅ$^{-3}$ and (0.0,0.443,0.471) with a height of 9.52(2)eÅ$^{-3}$. Anisotropic refinement including these Ag(3) and Tl(2) positions, respectively, converged to $R_1 = 0.070$ and $R_2 = 0.073$.

It is easy to distiguish $Ag^+$ from $Tl^+$ ions for several reasons. First, their atomic scattering factors are quite different, 46 $e^-$ for $Ag^+$ vs 80 $e^-$ for $Tl^+$. Secondly, their ionic radii are different, $Ag^+ = 1.26$Å and $Tl^+ = 1.47$Å.[28] Also, the approach distances between those ions and zeolite oxygens in dehydrated $Tl_{12}$-A[7,29] and partially decomposed $Ag_{12}$-A[17] have been determined and are indicative. Finally, the requirement that 12 metal atoms or ions be found limits the assignment of ionic identities.

**Table 3. Selected Interatomic Distances(Å) and Angles (deg)**

| | Crystal 1 | Crystal 2 | Crystal 3 | Crystal 4 |
|---|---|---|---|---|
| (Si,Al)-O(1) | 1.651(4) | 1.636(6) | 1.647(5) | 1.655(4) |
| (Si,Al)-O(2) | 1.660(6) | 1.649(8) | 1.647(8) | 1.653(9) |
| (Si,Al)-O(3) | 1.680(7) | 1.685(6) | 1.687(4) | 1.689(4) |
| Ag(1)-O(3) | 2.274(8) | 2.22(2) | 2.251(8) | 2.215(8) |
| Ag(2)-O(3) | | 2.50(1) | 2.34(1) | 2.654(9) |
| Ag(3)-O(3) | 2.85(2) | 2.77(2) | 2.89(1) | 2.84(2) |
| Tl(1)-O(3) | | | 2.59(1) | 2.705(5) |
| Tl(2)-O(2) | 2.795(8) | 2.747(9) | 2.767(6) | 2.752(8) |
| **Ag(4)-O(1)** | **2.82(3)** | | | |
| Ag(4)-O(2) | 2.29(3) | | | |
| Ag(1)-Ag(3) | 3.345(2) | 3.285(3) | 3.14(3) | 3.294(3) |
| Ag(3)-Ag(3) | 2.93(3) | 2.99(3) | 2.89(2) | 2.86(2) |
| O(1)-(Si,Al)-O(2) | 108.5(5) | 109.9(7) | 109.7(6) | 107.6(6) |
| O(1)-(Si,Al)-O(3) | 110.8(4) | 111.4(5) | 110.3(4) | 112.4(4) |
| O(2)-(Si,Al)-O(3) | 108.3(2) | 107.4(3) | 107.4(2) | 107.5(2) |
| O(3)-(Si,Al)-O(3) | 110.1(4) | 109.2(5) | 111.8(3) | 109.2(3) |
| (Si,Al)-O(1)-(Si,Al) | 151.4(9) | 154(1) | 152.2(2) | 151.3(9) |
| (Si,Al)-O(2)-(Si,Al) | 155.6(4) | 155.5(7) | 157.1(4) | 154.0(4) |
| (Si,Al)-O(3)-(Si,Al) | 143.5(5) | 141.4(7) | 142.5(5) | 140.9(5) |
| O(3)-Ag(1)-O(3) | 119.8(2) | 119.9(2) | 120.0(2) | 120.0(2) |
| O(3)-Ag(2)-O(3) | | 100.5(2) | 112.5(4) | 92.6(1) |
| O(1)-Ag(4)-O(2) | 57.7(4) | | | |
| O(3)-Tl(1)-O(3) | | | 97.6(2) | 90.3(2) |
| O(1)-Tl(2)-O(2) | 52.5(1) | 55.5(3) | 55.7(1) | 51.4(2) |
| Ag(1)-Ag(3)-Ag(1) | 89.59(7) | 89.79(9) | 89.57(6) | 89.5(1) |

Numbers in parentheses are estimated standard deviations in the units of the last significant digit given for the corresponding value.

At this point, a Fourier function revealed a peak at (0.072, 0.0415,0.415) with a height of 1.4(1)Å.$^{-3}$ Simultaneous positional, thermal and occupancy refinement including this position, Ag(4), converged at $R_1 = 0.054$ and $R_2 = 0.057$. All shifts in the final cycles of least squares were less than 3% of their corresponding esd's.

Crystal 2. Least-squares refinement began using the framework positions found in the structure of crystal 1. Refinement with anisotropic thermal parameters converged to $R_1 = 0.455$ and $R_2 = 0.416$. A difference Fourier synthesis revealed a large and distinct peak at (0.193,0.193,0.193) with a height of 10.2(3)eÅ$^{-3}$. Anisotropic refinement including this position, Ag(1), converged to $R_1 = 0.201$ and $R_2 = 0.187$. A subsequent difference synthesis revealed three peaks at (0.0,0.0,0.169), (0.0,0.443, 0.443), and (0.138,0.138,0.138) with heights of 5.6(3)eÅ$^{-3}$, 4.2(2)eÅ$^{-3}$, and 4.6(3)eÅ$^{-3}$, respectively. These were stable in least-squares refinement and anisotropic refinement including these positions, as Ag(3), Tl(2), and Ag(1), respectively, converged to $R_2 = 0.07$ and $R_1 = 0.07$. Additional information is given in Tables 1,2,3, and 4.

Crystal 3. Using the atomic parameters of the framework atoms, Ag(1), and Tl(1) in the structure of crystal 2, least-

**Table 4. Deviations of atoms(Å) from the (111) plane at O(3)**

| | Crystal 1 | Crystal 2 | Crystal 3 | Crystal 4 |
|---|---|---|---|---|
| O(2) | 0.224(5) | 0.246(7) | 0.183(5) | 0.268(5) |
| Ag(1) | 0.090(1) | 0.063(2) | 0.033(1) | 0.068(2) |
| Ag(2) | | -1.155(6) | -0.657(8) | -1.464(10) |
| Tl(1) | | | 1.287(5) | 1.554(1) |

A negative deviation indicates that the atom lies on the same side of the plane as the origin.

squares refinement was initiated. Anisotropic refinement of the framework atoms, Ag(1), and Tl(1) converged to $R_1$ = 0.333 and $R_2$ = 0.295. A difference Fourier synthesis revealed two peaks at (0.139,0.139,0.139) and (0.0,0.443,0.470) with heights of 3.6(2)eÅ$^{-3}$ and 10.9(2)eÅ$^{-3}$, respectively. Anisotropic refinement including these positions, Ag(2) and Tl(2), respectively, converged to $R_1$ = 0.121 and $R_2$ = 0.114. At this point, a difference Fourier synthesis revealed a peak at (0.0,0.0,0.166) with a height of 5.5(3)eÅ$^{-3}$. Final refinement including this position, Ag(3), converged to $R_1$ = 0.067 and $R_2$ = 0.076. Additional information is shown in Tables 1,2,3, and 4.

Crystal 4. Initial full-matrix least-squares refinement began with the framework atomic parameters, Ag(1), and Tl(1) from the structure of Crystal 3. Anisotropic refinement of the these atoms converged to $R_1$ = 0.338 and $R_2$ = 0.256. A difference Fourier synthesis revealed two peaks at (0.0, 0.443,0.471) and (0.0,0.0,0.166) with a height of 14.2(2)eÅ$^{-3}$ and 2.8(3)eÅ$^{-3}$, respectively. Refinement including these positions, Tl(2) and Ag(3), isotropically converged to $R_1$ = 0.197 and $R_2$ = 0.184. The ensuing anisotropic refinement converged to $R_1$ = 0.096 and $R_2$ = 0.086. A difference Fourier synthesis revealed a peak at (0.109,0.109,0.109) with a height of 6.7(2)eA$^{-3}$. This position, Ag(2), was stable in least-squares refinement and resulted in the final $R$ values $R_1$ = 0.063 and $R_2$ = 0.055. See Tables 1,2,3, and 4 for additional information.

The full-matrix least-squares program used in all structure determinations minimized $\Sigma\omega(F_o-F_c)^2$; the weight ($\omega$) of an observation was the reciprocal square of $\sigma(F_o)$ its standard deviation. Atomic scattering factors[30,31] for $Ag^0$, $Ag^+$, $O^-$, $Tl^+$, and $(Si,Al)^{1.75+}$ were used. The function describing (Si, Al)$^{1.75+}$ is the mean of the $Si^0$, $Si^{4+}$, $Al^0$, and $Al^{3+}$ functions. All scattering factors were modified to account for the real component ($\Delta f'$) of the anomalous dispersion correction.[32,33] See Tables 1,2,3, and 4 for additional information.

## Discussion

It appears that the order of depletion of $Ag^+$ positions (by reduction) is as follows (see Table 2): first, the cation associated with a 4-ring is reduced, then the three 8-ring ions, and finally at higher temperatures, the 6-ring ions replaced.[1,17]

The silver species at Ag(1) lie one threefold axes of the unit cell(see Figure 1), each nearly at the center of one of the eight 6-rings(see Table 4). These ions are at the same position as was found in dehydrated $Ag_{12}$-A[11] and partial $Tl^+$ exchanged zeolite A.[26,27] The distance between Ag(1) and its nearest framework oxygens, at O(3), is ca. 2.24Å (see Table 3). As compared to the sum of $Ag^+$ and $O^{2-}$ radii, 2.58 Å, this bond is quite short and therefore quite covalent. This indicates that the silver species at Ag(1) are the ions, $Ag^+$. Each

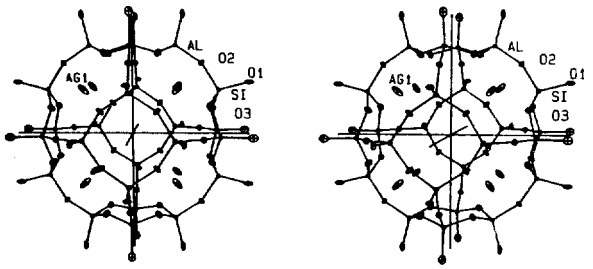


**Figure 1.** A stereoview of the sodalite unit of crystal 1. About 83% of the sodalite units have this arrangement. Ellipsoids of 20% probability are used.

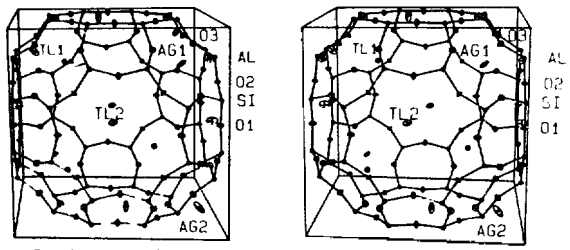


**Figure 2.** A stereoview of the large cavity of crystal 4 is shown using ellipsoids of 20% probability.

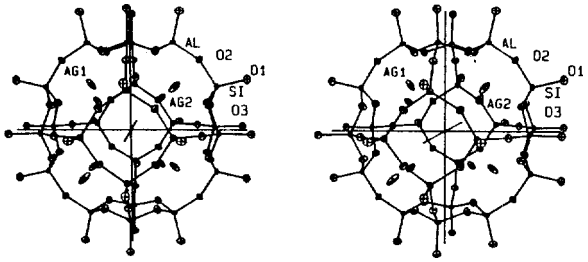


**Figure 3.** A stereoview of the sodalite unit of crystal 2.

$Ag^+$ ion at Ag(1) is trigonally coordinated to its respective set of three O(3) framework oxygens.

The silver species at Ag(2) are also located on threefold axes. These ions lie relatively far inside the sodalite cavity from the (111) plane at O(3) and are also trigonally coordinated to their respective sets of three O(3) framework oxygens (see Table 4 and Figure 2). The distance between Ag(2) and the nearest framework oxygens at O(3), ca. 2.50Å (see Table 3), indicates that the species at Ag(2) are ions, $Ag^+$.

The silver species at Ag(2) in the structure of crystal 2 are at positions similar to those found in previous studies (see Table 2). In this structure, about half of the unit cells have three $Ag^+$ ions at Ag(2) (See Table 2). They have been arranged in a triangular fashion within their low occupancy equipoint in order to maximize their intercationic distances: Ag(2)-Ag(2) = 4.57 Å (see Figure 3). Similar $Ag^+$ positions in $[Ag_3(H_2O)_3]^{3+}$ rings are found in the structure of hydrated $Ag_{12}$-A, and partially hydrated $Ag_{12}$-A. However, bridging oxygen atoms could not be located in this structure. This could be due to the low occupancy of that position.

The Ag(3) position is very similar to that of the neutral silver atoms in the structure of dehydrated $Ag_{12}$-A. The distance between Ag(3) and its nearest framework oxygens, again O(3), is much longer, ca. 2.83Å (see Table 3). This indicates that the silver species at Ag(3) are reduced silver atoms, $Ag^0$.

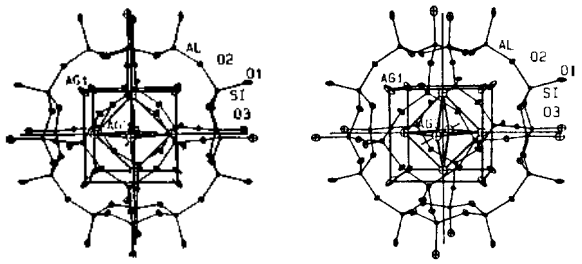


**Figure 4.** A stereoview of sodalite unit containing an$(Ag^+)_8$ $(Ag_6)$ cluster. The octahedral hexasilver molecule Ag(3) is stabilized by coordination to eight $Ag^+$ ions at Ag(2). About 17% of the sodalite cages in each four crystal structures probably have this arrangement. Ellipsodis of 20% probability are used.

The distance between Ag(1) and Ag(3) is ca. 3.31Å (see Table 3). This distance is equal to that of $Ag^\circ$-$Ag^\circ$ in the structure of dehydrated $Ag_{12}$-A. This distance, Ag(1)-Ag(3), is too short to be an unmoderated $Ag^+$-$Ag^+$ contact, and too long to be a $Ag^\circ$-$Ag^\circ$ bond. This is consistent with the conclusion (*vide supra*) that Ag(1) contains silver ions and Ag(3) silver atoms.

The distance between Ag(3) and Ag(3), ca. 2.92Å (see Table 3), is nearly equal to the $Ag^\circ$-$Ag^+$ distance, 2.89Å, found in silver metal[29], and is the same as that in the $(Ag^+)_8$ $(Ag_6)$ cluster. Accordingly and consistent with previous conclusion, the silver species at Ag(3) is a neutral silver atom, $Ag^\circ$.

In these four structures, only one $Ag^+$ ion per unit cell, that associated with a 4-ring is reduced. In the structures of crystals 2,3, and 4, the 8-ring positions are occupied by $Tl^+$ ions, which, because their ionic radius is larger, are more suited than $Ag^+$ ions to the large 8-ring sites (see Table 2). Accordingly, there are no $Ag^+$ ions at 8-ring sites except in crystal 1, and, apparently for that reason, more silver atoms are not generated. Although there is an $Ag^+$ ion at Ag(4) associated with the 8-ring in the structure of crystal 1 (see Table 2), $Ag_{10}Tl_2$-A, this $Ag^+$ ion was not reduced. This may be due to the relatively lower dehydration temperature, 350°C. In the crystal structure of fully dehydrated $Ag_{12}$-A, the number of the reduced silver atoms is more than one because the dehydration temperature was higher (395-475°C).

The reduction of $Ag^+$ to $Ag^\circ$ per unit cell proceeds by following reaction:

$$1/2\ H_2O + Ag^+ \longrightarrow 1/6\ Ag_6 + H^+ + 1/4\ O_2$$

This reduced Ag atom would have formed by autoreduction during the dehydration process. It is likely that a neutral $Ag_6$ cluster has formed in 1/6 of the sodalite units; the remaining 5/6 are empty of silver species (see Figures 4 and 1). This six atom cluster, subsequently verified by esr work[18-20] is stabilized by coordination to 8 $Ag^+$ ions near the centers of 6-rings, and may therefore be viewed as a $Ag_{14}^{8+}$ cluster (see Figure 4).

The $Tl^+$ ions at Tl(1) occupy threefold-axis positions near 6-rings, recessed ca. 1.42Å (see Table 4) into the large cavity from the(111) plane at O(3). The Tl(1)-O(3) distance is 2.59Å and 2.71Å in the study of crystal 3 and 4, respectively (see Table 3). The difference may be, in part, virtual; only a single "average" O(3) position is determined for each structure.

The three $Tl^+$ ions at Tl(2) are associated with 8-ring oxygens. These ions are located in the planes of the 8-oxygen rings, but not at their centers in order to make favorable approaches to the framework oxygens (see Table 2): The Tl(2)-O(2) distance is ca. 2.76Å and Tl(2)-O(1) is ca. 2.88Å (see Table 3).

The ionic radius of $Tl^+$, 1.47Å, is larger than that of $Ag^+$, 1.26Å. From a consideration of ionic radii, one would expect the larger $Tl^+$ ions to associate with the larger rings, the 8-ring. This consideration is affirmed by the present study.

A comparison of four structures determined in this work shows that, the first three $Tl^+$ ions to enter each unit cell prefer to associate with the larger 8-oxygen rings, and that additional $Tl^+$ ions are found on threefold axes deep inside of large cavity. Most $Ag^+$ ions are found on threefold axes nearly on the planes of 6-rings. Only the one $Ag^+$ ion per unit cell which is located at the least favorable position is reduced. The neutral silver atoms produced probably form an $Ag_6$ cluster in a fraction of the sodalite cages.

**Acknowledgements.** This work was supported by the Korean Science and Engineering Foundation. Special thanks are due Professor Karl Seff of University of Hawaii at Honolulu for his careful review of the manuscript and helpful suggestions.

## References

1. Y. Kim and K. Seff, *J. Phys. Chem.*, **82**, 1071 (1978).
2. Y. Kim and K. Seff, *J. Am. Chem. Soc.*, **100**, 6989 (1978).
3. P. C. W. Leung, K. B. Kunz, and K. Seff, *J. Phys. Chem.*, **79**, 2157 (1975).
4. R. L. Firor and K. Seff, *J. Am. Chem. Soc.*, **99**, 6249 (1977).
5. R. L. Firor and K. Seff, *J. Am. Chem. Soc.*, **98**, 5031 (1976).
6. T. B. Vance, Jr. and K. Seff, *J. Phys. Chem.*, **79**, 2163 (1975).
7. R. L. Firor and K. Seff, *J. Am. Chem. Soc.*, **99**, 4039 (1977).
8. R. Y. Yanagida, T. B. Vance, Jr., and K. Seff, *J. Chem. Soc. D.*, 382 (1973).
9. A. A. Amaro, C. L. Kovaciny, K. B. Kunz, P. E. Riley, T. B. Vance, Jr., R. Y. Yanagida, and K. Seff, "Proceedings of the Third International Conference on Molecular Sieves", Leuven University Press, Belgium, 1973, pp 113-118.
10. P. E. Riley and K. Seff, *J. Chem. Soc. D.*, 1287 (1972).
11. P. E. Riley and K. Seff, *Inorg. Chem.*, **13**, 1355 (1974).
12. P. E. Riley and K. Seff, *J. Phys. Chem.*, **79**, 1594 (1975).
13. N. V. Raghavan and K. Seff, *J. Phys. Chem.*, **80**, 2133 (1976).
14. K. Seff, Ph. D., Thesis, Massachusetts Institute of Technology, 1964.
15. R. L. Firor and K. Seff, *J. Am. Chem. Soc.*, **99**, 7059 (1977).
16. A discussion of the structure and of the nomenclature used to discuss zeolite A is available. (a) R. Y. Yanagida, A. A. Amaro, and K. Seff, *J. Phys. Chem.*, **77**, 805 (1973); (b) L. Broussard and D. P. Shoemaker, *J. Am. Chem. Soc.*, **82**, 1041 (1960); (c) K. Seff, Acc. Chem. Res., **9**, 121 (1976).
17. Y. Kim and K. Seff, *J. Am. Chem. Soc.*, **99**, 7055 (1977).
18. D. Hermerschmidt and R. Haul, *Ber. Bunsenges Phys. Chem.*, **84**, 902 (1980).
19. P. J. Grobet and R. A. Schoonheydt, *Surf. Sci.*, **156**, 893 (1985).

20. J. R. Morton and K. P. Preston, *J. Magn. Resonance*, **68**, 121 (1986).
21. J. F. Charnell, *J. Cryst. Growth*, **8**, 291 (1971).
22. K. Seff, *J. Phys. Chem.*, **76**, 2601 (1972).
23. K. Seff and M. D. Mellum, *J. Phys. Chem.*, **88**, 3560 (1984).
24. R. E. Riley and K. Seff, *J. Am. Chem. Soc.*, **95**, 8180 (1973).
25. B. A. Frenz and Y. Okaya, Structure Determination Package, Version 1.2.0(1985), Enraf-Nonius, Delft (Holland).
26. Y. Kim and K. Seff, *J. Am. Chem. Soc.*, **100**, 178 (1978).
27. This nomenclature refers to the contents of the unit cell. For example, $Ag_6Tl_6$-A represents $Ag_6Tl_6Al_{12}Si_{12}O_{48}$, exclusive of guest molecules which may be present, such as water.
28. "Handbook of Chemistry and Physics", 55th ed., Chemical Rubber Co., Cleveland, Ohio, 1974, p F-198.
29. P. E. Riley and K. Seff, *J. Phys. Chem.*, **76**, 2593 (1972).
30. P. A. Dole and P. S. Turner, *Acta Crystallogr., Sect. A.*, **24**, 390 (1968).
31. "International Tables for X-Ray Crystallography", Vol. IV; Kynoch Press; Birmingham, England, 1974; pp. 73-87.
32. D. T. Cromer, *Acta Crystallogr.*, **18**, 17 (1965).
33. Reference 31, pp. 149-150.

# Surfactant Effect on the Hydrophobic Interaction between Rhodamine 6G and Sodium Tetraphenylborate

**Sae-Yung Oh, Beom-Gyu Lee, and Kang-Jin Kim***

*Department of Chemistry, Korea University, Seoul 136-701.* *Received April 28, 1988*

The hydrophobic interaction occurring between rhodamine 6G and tetraphenylborate was investigated spectroscopically by varying the medium with the addition of surfactants or ethanol. The ion aggregates formed between the two ions were destroyed by the additives. The dye existed as monomeric species in the presence of a cationic surfactant whereas it was incorporated with anionic and nonionic surfactants. For the complete dissociation more than the critical micelle concentration (cmc) was required with a nonionic surfactant while less than cmc was necessary with the others.

## Introduction

The absorption spectra of aqueous solutions containing dye cations and hydrophobic anions, such as tetraphenylborate ($TPB^-$), show spectral changes conspicuously at longer wavelengths with respect to dye blank due to the association of dye and anion.[1-5] When both cation and anion are large, univalent, and poorly hydrated, water structure forces the two ions to form an ion-pair to minimize their disturbance to itself and to maximize water-water binding.[6] The opposite charges assuredly facilitate the association. The tendency of water molecules to self-associate should be responsible for the ion-pairing. Thus the factors which could modify the tendency should be likely to influence the formation of ion-pairs. The addition of 1,4-dioxane or urea, which decreases or increases the dielectric constant of medium, respectively, is found to interfere with the formation of ion-pairs and eventually to destroy completely the ion-pairs into single ions.[7]

The widespread use of dyes, such as rhodamine B, rhodamine 6G, and acridine red, in tunable lasers has stimulated a number of studies on spectroscopic and structural properties in relation to the lasing mechanism.[8,9] Since many of the commonly used dyes tend to aggregate and form dimers in solution, most of studies have been concerned with understanding the spectral effects particularly blue shifts in the absorption spectra produced by dimerization.[9,10] However, spectral changes attributed to hydrophobic interaction have attracted little attention, insofar as we are aware, despite the fact that theoretical treatments of dimer spectra give predictions regarding the red shifts.

Many peculiarities have been found in the spectroscopic properties of dyes with a detergent around cmc. The studies of fluorescence decay and the analysis of absorption bands of pinacyanol[11] and cyanine dyes[3,12] with sodium dodecyl sulfate (SDS) and of rhodamine 6G ($Rh6G^+$) with SDS[13] were carried out to clarify the nature of the interaction between dye and detergent. Again, in these studies hydrophobic interactions were largely neglected.

In the present paper therefore the absorption and fluorescence emission behaviors of $Rh6G^+$ and $TPB^-$ mixed solutions are reported in the presence of a surfactant for the purpose of understanding the nature of hydrophobic interaction between the two ions. Cetyltrimethylammonium bromide (CTAB), SDS, or Triton X-100 (TX-100) was used as a cationic, anionic, or nonionic surfactant. Since the absorption spectrum of dye and the formation of micelle are greatly influenced by the pH and ionic strength of the medium, respectively, the two variables are necessarily controlled.[8,14]

## Experimental

Rhodamine 6G (Aldrich) and sodium tetraphenylborate (Fluka) of reagent grade as sources of cation, $Rh6G^+$, and of anion, $TPB^-$ respectively were dissolved in distilled water and stored in polyethylene bottles. All solutions containing $Rh6G^+$ were wrapped with aluminum foil to prevent photodissociation. TX-100 (Shinyo Pure Chemicals), SDS and